Pharmaceutical Research, Vol. 25, No. 4, April 2008 (© 2007)
DOI: 10.1007/s11095-007-9444-8

Research Paper

Molecular Mobility, Thermodynamics and Stability of Griseofulvin's Ultraviscous and Glassy States from Dynamic Heat Capacity

E. Tombari,[1] S. Presto,[1] G. P. Johari,[2,4] and Ravi M. Shanker[3]

Received May 28, 2007; accepted August 24, 2007; published online September 27, 2007

Purpose. To determine the calorimetric relaxation time needed for modeling griseofulvin's stability against crystallization during storage.
Methods. Both temperature-modulated and unmodulated scanning calorimetry have been used to determine the heat capacity of griseofulvin in the glassy and melt state.
Results. The calorimetric relaxation time, τ_{cal}, of its melt varies with the temperature T according to the relation, $\tau_{cal}[s] = 10^{-13.3} \exp[2,292/(T[K] - 289.5)]$, and the distribution of relaxation times parameter is 0.67. The unrelaxed heat capacity of the griseofulvin melt is equal to its vibrational heat capacity.
Conclusions. Griseofulvin neither crystallizes on heating to 373 K at 1 K/h rate, nor on cooling. Molecular mobility and vibrational heat capacity measured here are more reliable for modeling a pharmaceutical's stability against crystallization than the currently used kinetics–thermodynamics relations, and molecular mobility in the (fixed structure) glassy state is much greater than the usual extrapolation from the melt state yields. Molecular relaxation time of the glassy state of griseofulvin is about 2 months at 298 K, and longer at lower temperatures. It would spontaneously increase with time. If the long-range motions alone were needed for crystallization, griseofulvin would become more stable against crystallization during storage.

KEY WORDS: calorimetric relaxation time; complex heat capacity; glassy state; griseofulvin; stability.

INTRODUCTION

The Gibbs free energy of a non-crystalline solid pharmaceutical is greater than that of its crystalline form, and therefore its saturation solubility and hence the bioavailability is higher. This is the basis on which procedures for improving the bioavailability of poorly soluble pharmaceuticals are currently being developed. It is also known that non-crystalline states of different free energies of a pharmaceutical are produced by different techniques. Therefore, bioavailability of a given pharmaceutical varies with the method of its industrial production, such as lyophilization (freeze-drying), flocculation (precipitation with an external agent usually an ionic polymer), trituration (high-speed mechanical deformation) and vitrification by supercooling the melt. It also varies with time during storage as the non-crystalline state structurally relaxes and/or slowly crystallizes. Consequently its net free energy and bioavailability decreases.

Long-range molecular diffusion over a time scale of days or longer occurs in a non-crystalline solid. It is believed that these diffusive motions lead to crystal nucleation and growth, which reduces the free energy and hence the saturation solubility. Therefore, molecular mobility is currently used for modeling a pharmaceutical's stability against crystallization and chemical reactions (1–8). In such models, the temperature dependence of the relaxation time (inverse of molecular mobility) of a supercooled melt is determined by using a relation (9) between the relaxation time and the extrapolated excess entropy of the melt over the crystal phase, S_{exc} (10), and it is assumed that this S_{exc} would become zero at an unattainable equilibrium condition in the glassy state (9,10). Moreover, correlations between the relaxation time and heat capacity are used in such modeling (11–15). All these add to the uncertainty in the prediction of a pharmaceutical's stability against crystallization.

As part of our studies of pharmaceuticals in the glassy state (16), we have determined the temperature dependence of the molecular mobility in griseofulvin, and estimated its stability against crystallization by measuring the dynamic heat capacity in three conditions, (1) during its melt's extremely slow cooling at 1 K/h rate to temperatures low enough that the molecular relaxation time could be determined to values longer than 10^4 s, and (2) during the extremely slow subsequent heating of its glassy state at the same rate until the glass became an ultraviscous melt. This is reported here. The method eliminates the use of correlations between other relaxation times and the heat capacity. We

[1] Istituto per i Processi Chimico-Fisici del CNR, 56124, Pisa, Italy.
[2] Department of Materials Science and Engineering, McMaster University, Hamilton, Ontario L8S 4L7, Canada.
[3] Groton Laboratories, Pfizer Inc., Groton, Connecticut 06340, USA.
[4] To whom correspondence should be addressed. (e-mail: joharig@mcmaster.ca)

also report the time-dependent or apparent heat capacity, $C_{p,app}$, of griseofulvin studied during cooling at a much slower rate of 20 K/h until it vitrifies and then during the heating of its glassy state at the same rate. Finally, we provide a method for determining the true relaxation time and its increase during griseofulvin's storage and use it to predict its stability against crystallization at 298 K.

The purpose of the study is not for understanding the formation of glassy state and its crystallization. Rather, it is for determining the relaxation time needed for modeling a pharmaceutical's stability against crystallization during storage. As before (16), we avoid using both the currently debated kinetic-thermodynamic correlations and the misleading (popular) terms in the literature on supercooled liquids, such as fragility (17). A critical appraisal of their use has appeared in a report on the dielectric study of acetaminophen (18).

DYNAMIC HEAT CAPACITY AND RELAXATION

Since the method used in this study is new to most pharmaceutical researchers, it seems appropriate to describe briefly its general concept, data analysis and interpretation: Dynamic heat capacity refers to the frequency-dependent part of the heat capacity C_p measured by sinusoidally modulating the temperature of a material. It is a complex quantity, $C_p^*\left(=C_p'-iC_p''\right)$, where C_p' and C_p'' are the real and imaginary components of C_p^* and $i=(-1)^{1/2}$. C_p' oscillates in phase with the temperature, and C_p'' oscillates out of phase during the course of one temperature modulation cycle. The theory and the method for C_p' and C_p'' measurements have been well founded and reviewed extensively (19,20), and the related formalisms have been provided earlier (16,21–23). Briefly, the temperature of the sample is sinusoidally modulated (oscillated) at a fixed frequency, ω_{mod}, and the amount of heat stored and heat released that reverses with reversal of the temperature in the modulation cycle is measured. These yield the amplitude and phase angle from which C_p' and C_p'' are calculated. A data point obtained for each cycle is assigned to the mean temperature of the modulation period, and the measured C_p' and C_p'' refer to this mean temperature. The initial state of the sample is attained within one temperature modulation cycle when the C_p' and C_p'' values measured during the cooling at a fixed rate are found to coincide with the C_p' and C_p'' values measured during the heating at the same rate.

The equilibrium quantities and τ_{cal} are determined by analyzing the C_p' and C_p'' data in a manner analogous to the analysis of the real and imaginary components of the complex mechanical modulus and complex dielectric permittivity. When measurements are made at low ω_{mod} and/or high temperatures, C_p'' is formally zero or negligibly small, and C_p' is equal to $C_{p,0}$, the limiting low-frequency, or the equilibrium value. In such conditions, the product $\omega_{mod}\tau_{cal}$ approaches zero, where τ_{cal} is the characteristic calorimetric relaxation time (to distinguish it from other structural relaxation times, which differ in meaning and mechanism, we use the term τ_{cal} here). When measurements are made at high ω_{mod} and/or low temperatures, C_p'' is also zero or negligibly small, and in this case the measured C_p' is equal to $C_{p,\infty}$, the limiting high-frequency C_p of a relaxation process. In such conditions, $\omega_{mod}\tau_{cal}$ is much higher, approaching infinity. Thus $C_{p,\infty}$ is the unrelaxed and $C_{p,0}$ is the relaxed value of C_p. Over the temperature range in which $C_{p,\infty}$ increases to $C_{p,0}$, the plot of C_p' against the temperature at a fixed ω_{mod} has the shape of a stretched sigmoid, and C_p'' shows a peak. The relaxation strength of dynamic C_p is, $\Delta C_{p,\alpha}=C_{p,0}-C_{p,\infty}$. It corresponds to molecular motions of the α-relaxation process that determine the viscosity of the melt, and therefore all calorimetric relaxation features are for the α-relaxation process. The temperature at which the C_p''-peak appears is the temperature at which τ_{cal} is equal to the reciprocal of the angular frequency of temperature modulation. Note that there is an important distinction between the dynamic C_p and dielectric and mechanical relaxation measurement. In the dynamic C_p measurements, modulation of a material's temperature itself changes the molecular mobility, $C_{p,0}$ and $C_{p,\infty}$. But an oscillating electric field and mechanical stress do not do so in a linear response range. Since the molecular mobility, $C_{p,0}$ and $C_{p,\infty}$ vary nonlinearly with the temperature, they do not vary symmetrically about the mean temperature of the (sinusoidal) temperature modulation, and thus have an effect on the data analysis. A critical appraisal has shown that the effect of this variation is negligibly small (24,25).

In general, $C_{p,0}$ of a melt is the sum of contributions from molecular vibrations and mobility, all of which decrease on cooling. In contrast, C_p' and $C_{p,app}$ of the glassy state are the sum of contributions mainly from vibrations, with two small contributions from molecular kinetics, one from localized motions of the JG relaxation (26–31) and the second from the kinetically unfrozen faster modes in the distribution of the α-relaxation process (28–31). These contributions decrease during storage as the glass structure relaxes spontaneously to a state of lower fictive temperature T_f (the temperature at which the glass and the liquid have the same properties) volume, enthalpy and entropy (32–36) because the vibrational frequency increases, the vibrational amplitude, the α-relaxation contribution and the JG relaxation contribution decrease—the decrease in the last one due to decrease in the number of molecules involved in localized motions (34–42). The glassy state formed by slow cooling has a lower T_f and hence a lesser JG relaxation contribution to C_p than that formed by normal cooling (33–42).

The dynamic heat capacity at a temperature T measured for a fixed ω_{mod} is given by (23,29–31,43),

$$C_p'(T)=C_{p,\alpha}'(T)+\Delta C_{p,JG}(T)+C_{p,\mathrm{vib}}(T)+C_{p,\mathrm{anh}}(T), \quad (1)$$

where $C_{p,\alpha}'$ is the contribution from the α-relaxation process, whose magnitude is reversible in the time period of sinusoidal modulation and decreases with increase in ω_{mod} (19,20). The quantity $\Delta C_{p,JG}$ is the full contribution from the JG relaxation, which kinetically freezes on cooling of the glass to T far below T_g, and even below T_k at which the extrapolated excess entropy, S_{exc}, is taken to be zero, an extrapolation that is now seen as implausible (43–47). The JG relaxation is found to kinetically unfreeze on heating in a temperature range below T_g and even below T_k (48–50). $C_{p,vib}$ is the vibrational contribution and $C_{p,anh}$ the anharmonic force contribution. All the four contributions to C_p' decrease with decrease in T until the liquid vitrifies, but do not change with time. After vitrification, C_p' contains contributions from

(1) localized molecular motions of the JG relaxation found in both the vitrified and melt state by dielectric and mechanical relaxation spectroscopy (26,37,38,51), (2) molecular vibrations including the effect of anharmonic forces (27,28), and (3) kinetically unfrozen, faster modes in the distribution of relaxation times of the α-relaxation process (29–31). Its magnitude is negligibly different from $C_{p,\infty}$.

As the non-equilibrium structure of vitrified state relaxes during storage, C_p' in Eq. 1 decreases with time partly because τ_{cal} increases, which decreases C_p', α and partly because $\Delta C_{p,JG}$, $C_{p,vib}$ and $C_{p,anh}$ decrease. When the glassy state is heated, C_p', α in Eq. 1 increases because τ_{cal} decreases. If structural relaxation also occurs, $\Delta C_{p,JG}$, $C_{p,vib}$ and $C_{p,anh}$ first irreversibly decrease and then reversibly increase after the equilibrium melt state has been reached over the temperature modulation period.

The plots of C_p' and C_p'' against the temperature are used to calculate τ_{cal} Briefly, the equations used are (16),

$$C_p^*(\omega, T) = C_p'(\omega, T) - iC_p''(\omega, T) \tag{2}$$

$$C_p^*(\omega, T) = C_{p,\infty}(T) + \left[C_{p,0}(T) - C_{p,\infty}(T)\right] \int_o^\infty -e^{-i\omega t}\left(\frac{\partial \phi(t)}{\partial t}\right)_T dt \tag{3}$$

where t refers to the time for the observation of the decay of a response after removal of an applied stress at a fixed temperature T, ϕ is the relaxation function, ω is the modulation frequency in radians and $C_{p,0}$ and $C_{p,\infty}$ are as described above. Equation 3 is valid only when T remains constant. But it is still valid, albeit with negligible error, when T increases by a small extent during the time taken to measure C_p^* (this error is present also in the adiabatic calorimetry measurements of C_p, as the liquid's structure changes when a known amount of the heat input raises the sample's temperature by 0.5 to 1 K). For this condition,

$$[\phi(t)]_T = \exp\left[-\left(\frac{t}{\tau_{cal}}\right)^\beta\right]_T \tag{4}$$

where t is the same as in Eq. 2, τ_{cal} is the characteristic *calorimetric* relaxation time which is invariant of t, β is an empirical parameter whose magnitude determines the shape of the spectra. For β=1, the relaxation spectrum has a single relaxation time, and for $0<\beta<1$ the relaxation spectrum is asymmetrically broadened more at the high-frequency than at the low-frequency side. To restate, C_p' and C_p'' may be measured accurately only when the temperature change is insignificant during the course of the measurement, or that the effect of such changes on the equilibrium and dynamic properties is negligible in comparison with the measurement errors. Hence, Eq. 3 becomes,

$$C_p^*{}_{,norm}[\omega\tau(T)] = \int_o^\infty -e^{-i\omega t}\left(\frac{\partial \phi(t)}{\partial t}\right)_T dt \tag{5}$$

or, $\left[C'_{p,norm} - i\,C''_{p,norm}\right] = L(\partial\phi/\partial t)_T$, where, $C'_{p,norm} = \left(C_p' - C_{p,\infty}\right)\Big/\left(C_{p,0} - C_{p,\infty}\right)$, $C''_{p,norm} = C_p''\Big/\left(C_{p,0} - C_{p,\infty}\right)$ and the notation L represents the Laplace transform. Both $C'_{p,norm}$, and $C''_{p,norm}$ are functions of the product $\omega\tau_{cal}(T)$. Therefore,

$$C_p'(T) = C_{p,\infty}(T) + \left[C_{p,0}(T) - C_{p,\infty}(T)\right] C'_{p,norm}(\omega\tau_{cal}(T)) \tag{6}$$

and,

$$C_p''(T) = \left[C_{p,0}(T) - C_{p,\infty}(T)\right] C''_{p,norm}(\omega\tau_{cal}(T)) \tag{7}$$

Thus Eqs. 6 and 7 become invariant of one's choice of either T or τ_{cal} and each data point for a single frequency measurement is described by $\left[C_{p,0}(T) - C_{p,\infty}(T)\right]$, $\beta(T)$ and $\omega\tau_{cal}(T)$. Thus, the Kramers–Kronig relation for a dissipation-relaxation process is obeyed. On the approximation that the parameter β does not vary with T, τ_{cal} is determined from the complex plane plot of $C''_{p,norm}$ against $C'_{p,norm}$ in which each data point corresponds to the variable $\omega\tau_{cal}$, as in the usual complex plane plots constructed from spectroscopy data for a fixed T for which τ_{cal} is fixed and ω is varied.

Finally, the variation of τ_{cal} of an ultraviscous melt with T generally consists of two parts: The first part is from the temperature variation alone. It follows an Arrhenius equation, $\tau_{cal} \propto \exp\left(E_{Arrh}/RT\right)$ where E_{Arrh} is the Arrhenius energy and R the gas constant. Accordingly, the plot of $\log_{10}\tau_{cal}$ against $1/T$ is linear with a slope of $E_{Arrh}/2.303R$ and its intercept or limiting high temperature τ_{cal} corresponds to the vibrational time scale or phonon frequency of $\sim 10^{-14}$ s. The second part is from the melt's changing structure with changing T, as known from early x-ray diffraction studies, and more clearly observed in a neutron diffraction study of propylene glycol (52). The rate at which a melt's structure changes increases progressively more rapidly with decrease in T. Consequently, τ_{cal} of an ultraviscous melt becomes progressively longer on cooling and its plot against $1/T$ deviates progressively more from the Arrhenius equation. In the glassy state, the structure does not change with changing T, and τ_{cal} varies according to the Arrhenius equation, as is known from earlier studies (32,53–57).

EXPERIMENTAL METHODS

Micronized fine crystalline powder of griseofulvin of 99 + % purity was purchased from Sigma-Aldrich Chemicals, and used as such. It is derived from the mold *Penicillium griseofulvum*, and its chemical name is (2*S*,6′*R*)-7-chloro-2′,4,6-trimethoxy-6′-methyl-3*H*, 4′*H*-spiro[1-benzofuran-2,1′-cyclohex[2]ene]-3,4′-dione ($C_{17}H_{17}ClO_6$, mol wt 352.77 Da). The pharmaceutical is used for treating dermatophytosis and is administered in microcrystalline state, which enhances its absorption, in the tablet form or in the liquid form. It is taken orally and also used topically. Griseofulvin does not seem to form intermolecular hydrogen bonds in the pure state or with chain segments of poly(vinyl pyrrolidone) when mixed with it (58). It has been reported that milling of griseofulvin increases its aqueous solubility (59).

Dynamic heat capacity measurements were performed by using the technique of temperature-modulated scanning

calorimetry (TMSC). In this technique, a sinusoidal modulation of a predetermined frequency and temperature amplitude is superposed on the temperature–time profile of a sample, and the complex heat capacity or equivalently C_p' and C_p'' are determined. The technique has been used for studies in the quasi-isothermal mode when the average temperature is kept fixed, and in a temperature scanning mode in which the temperature is programmed to increase or to decrease linearly with time. The calorimeter, described elsewhere (60), has been used for studying the denaturation process of lysozyme (21), the isomerization thermodynamics of fructose (22), the kinetics of polymerization process (61), the decrease in C_p on structural relaxation of a polymer (23), the endothermic freezing and exothermic melting of a mixture of α-cyclodextrin, 4 methylpyridine and water (62), the position-dependent energy of water molecules in nanopores (63), the formation of an ice clathrate (64), the HCl catalyzed sucrose hydrolysis (65), the spontaneous melting of fructose (66) and the dynamic heat capacity of acetaminophen (16). These studies have shown that TMSC is unique for investigating the thermodynamics simultaneously with molecular kinetics of also those phenomena that can not be studied by normal calorimetry, dielectric and mechanical relaxation or by NMR methods.

Griseofulvin was studied in the temperature-scanning mode and measurements were made during both cooling and heating. The temperature modulation frequency ω_{mod} was 3.33 mHz or 20.9 mrad/s, i.e., the time period of a sinusoidal oscillation t_{mod} was 300 s (5 min), and the peak to peak temperature modulation amplitude was 1 K. Since we use a low modulation frequency to determine τ_{cal}, the heating and cooling rates used for scanning had to be much lower than those used for the usual calorimetric experiments. Therefore, the rates used are 1 K/h (0.0166 K/min).

In the TMSC assembly, the sample is contained in a glass capillary of 2.2 mm internal diameter, 0.3 mm thick-wall closed at one end. The smooth glass surface provides few or no sites for heterogeneous nucleation. In a typical experiment, griseofulvin powder in nominal amount of 200 mg was carefully transferred into this capillary in a dry atmosphere, and its mass accurately determined. The open end of the capillary was closed by fusing with a directed thin flame and the sample was hermetically sealed. The sealed sample was completely melted by keeping it in a thermostat at 497 K for 5 min. It was then quenched in a methanol bath kept at 255 K and finally transferred to the sample cell of the calorimeter that had been isothermally kept at 370 K. It was kept at 370 K for 1.2 ks and then cooled to 335 K at a rate of 1 K/h. After keeping at 335 K for 1.2 ks, it was heated to 370 K at a rate of 1 K/h. The thermal cycle between 335 and 370 K was repeated. An analysis of such experiments has shown that when the time-scale corresponding to the temperature scanning rate is much greater than the relaxation time of a material, the errors in the derived quantities are insignificant (16,65). For 1 K/h scanning rate, this condition is fulfilled.

The calorimeter was calibrated by using dodecane and glycerol as standard liquids for C_p values, and the absolute C_p value of griseofulvin was determined. Measurements were repeated with different samples. Reproducibility of the C_p values for different samples was found to be better than 0.5%. Accuracy of the complex heat capacity modulus $\left(C_p'^2 + C_p''^2\right)^{1/2}$ was better then 0.5%, and the out of (sinusoidal) phase C_p uncertainty was better than 3 mrad. This accuracy, the very slow average heating and cooling rates of 1 K/h and t_{mod} of 300 s allowed us, (1) to determine C_p* of the sample by maintaining it in a thermodynamic equilibrium for most of the temperature interval in which C_p'' remained significant, (2) to ascertain that the finite and significant C_p'' value measured was due to the heat capacity relaxation, and (3) to yield highly accurate values of C_p' and C_p'' for determining the temperature dependence of the characteristic relaxation time values from 1 s to 10 ks. Thus griseofulvin was investigated in an important temperature range in which its ultraviscous liquid vitrified on cooling and its glass softened to an ultraviscous liquid on heating.

Prior to performing the C_p* measurements, the time-dependent apparent heat capacity, $C_{p,app}$, of griseofulvin was measured (without temperature-modulation) by cooling at 20 K/h rate, and then heating at the same rate. This $C_{p,app}$ is the same quantity that is measured in differential scanning calorimetry (DSC) during heating at a much higher rate of 10 to 30 K/min. This allowed us to determine not only the relaxation characteristics obtainable from the usual scanning calorimetry, but also the temperature range over which griseofulvin melt did not crystallize. In summary, the $C_{p,app}$ measurements were performed during heating and cooling at 20 K/h rate and C_p' and C_p'' measurements were performed during both cooling and heating at 1 K/h rate.

RESULTS AND ANALYSIS

The measured $C_{p,app}$ of griseofulvin is plotted against T in Fig. 1A. Here, the squares denote the values measured during the cooling of the ultraviscous melt at 20 K/h from 373.2 to 253.2 K and the circles denote the values measured thereafter on heating the glass from 253.2 to 373.2 K also at 20 K/h rate. These show that $C_{p,app}$ decreases in a sigmoid-shape manner on cooling and increases in a sigmoid-shape manner on heating, both through the temperature range of 345–365 K. This shape is characteristic of gradual kinetic freezing during vitrification of the melt on cooling and kinetic unfreezing during the softening of the glass on heating, and is a manifestation of the time- and temperature-dependent loss of the equilibrium state structure during the cooling and of recovery of the equilibrium structure during the heating. The $C_{p,app}$ overshoot in the heating curve in Fig. 1A, as in the usual DSC scan, is due to rapid recovery of the enthalpy after the temperature of the equilibrium-line has been crossed during heating and the state of lower enthalpy than the equilibrium value has been reached for a given heating rate. At low temperatures in Fig. 1A, $C_{p,app}$ measured during the cooling is greater than that measured during the heating, and at high temperatures it is higher. There is also a perceptible decrease in the $C_{p,app}$ value at T<350 K during the heating, which is due to the characteristic, spontaneous relaxation of the glassy state toward an entropically less disordered structure of lower volume, enthalpy and entropy (32,67). Since the cooling and heating rates of 20 K/h used here are 30 to 60-times slower than the rates of 10 K/min to 20 K/min used in the usual DSC

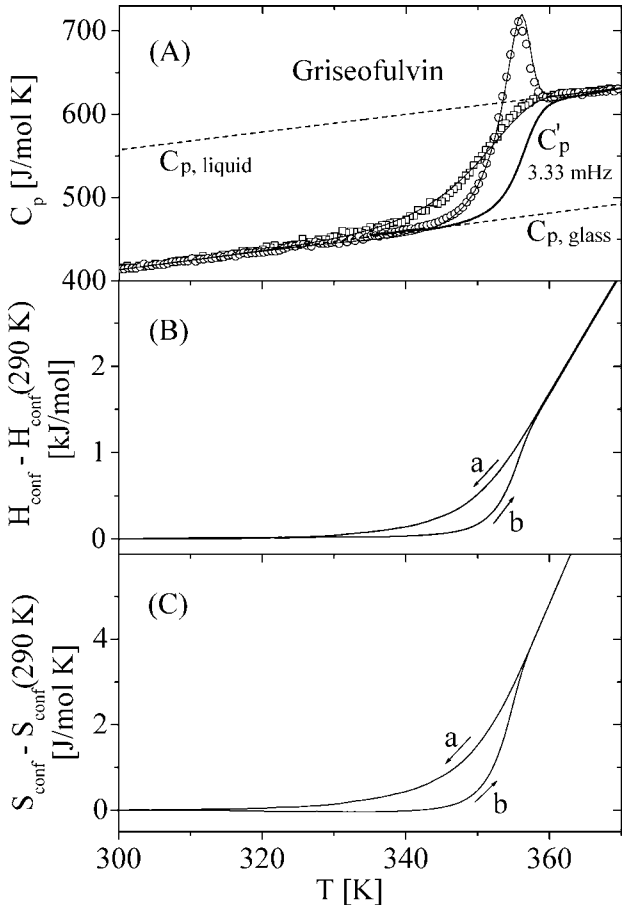

Fig. 1. **A** $C_{p,app}$ of griseofulvin measured during first cooling from 373.2 to 253.2 K at 20 K/h shown by *squares* and thereafter during heating from 253.2 to 373.2 K at 20 K/h rate, shown by *circles*. During heating $C_{p,app}$ shows an overshoot at 356.2 K and a hysteresis between the $C_{p,app}$ measured during cooling and that during heating. *Smooth lines* show the value of $C_{p,app}$ calculated by using the non-exponential, nonlinear structural relaxation with $\ln A = -170$, $\beta = 0.75$, $x = 0.45$ and $\Delta h^* = 516$ kJ/mol both during cooling and thereafter heating. Also shown is a plot of C_p', as indicated. **B** The configurational enthalpy of griseofulvin obtained from the area between the plot for $C_{p,app}$ and the plot for $C_p(\infty)$, as shown in (A). **C** The corresponding plots of the *configurational entropy*. Curve *(a)* is for cooling and *(b)* is for heating.

experiments, T_g determined from the onset temperature of the $C_{p,app}$ endotherm in Fig. 1A would be considerably less than the T_g determined from a usual DSC scan.

The manner in which the enthalpy and entropy of the melt decrease during cooling until the melt vitrifies, and increase during heating until the glass softens to an ultra-viscous melt are important in a pharmaceutical's study. This is especially so because both quantities indicate the manner of the time- and temperature-dependence of the thermodynamic functions, and the entropy has been used for modelling the stability of pharmaceuticals against crystallization (11–15,17). Therefore, the configurational enthalpy change for griseofulvin was determined by integrating the plot of the $[C_{p,app}(T) - C_{p,glass}]$ against T from $T = 290$ K and by taking $T = 290$ K as a reference temperature which is well below the griseofulvin's structural freezing temperature for the cooling and unfreezing temperature for heating both at 20 K/h rates. This yields the enthalpy difference $[H_{conf}(T) - H_{conf}(290\ \text{K})]$, which is plotted against T in Fig. 1B. Similarly, the entropy change $[S_{conf}(T) - S_{conf}(290\ \text{K})]$ was determined by integrating the plot of $[C_{p,app}(T) - C_{p,glass}]$ against $\ln T$, and it value is plotted against T in Fig. 1C. These plots are labeled as (a) for the cooling, and as (b) for the heating sequence of the measurements.

In general, the elbow-shape change in the slope of the enthalpy and of the entropy against T plots occurs when the melt's structure kinetically freezes on cooling or kinetically unfreezes on heating. For a typical heating rate of 10 K/min in the DSC experiments, the temperature at which the slope changes is defined as T_g. It is estimated from the point of intersection of two straight lines, one is an extension of the $C_{p,app}$ against T plot obtained by heating the glassy state as shown by circles in Fig. 1A, and the second is an extension from the point of inflexion of the sigmoid-shape rise in $C_{p,app}$. For cooling rates other than 10 K/min, this temperature is said to be the fictive temperature T_f (32). It is also the lowest temperature at which the liquid during cooling is in thermodynamic equilibrium. When the cooling rate is higher than 10 K/min, T_f is higher than T_g, and when the cooling rate is lower, T_f is lower than T_g. If the cooling rate is decreased, the inverted sigmoid shape curve would shift to lower temperatures and become narrower, and the glass formed would have a lower T_f. Although $C_{p,app}$, enthalpy and entropy against T plot should yield the same T_f, this temperature is more accurately defined by the enthalpy and entropy against T plots than by the $C_{p,app}$ against T plot. When no structural relaxation occurs, the glassy state is said to have a fixed T_f, but when structural relaxation occurs, its T_f changes with time.

For the 20 K/h cooling rate, T_f of griseofulvin is the temperature at which the slope of the plots labeled (a) for the enthalpy difference in Fig. 1B and the entropy difference in Fig. 1C changes (note that T_f has been inadvertently defined incorrectly in the plot of enthalpy or free volume against T in Fig. 1 of (14)). The values measured for the heating in Figs. 1B and 1C are less than those measured for cooling at $T < T_g$, which indicates that griseofulvin structurally relaxes and consequently its T_f decreases, even for such a low heating and cooling rates.

We now describe the results of the C_p' and C_p'' measurements performed over a temperature range of 335 to 370 K for ω_{mod} of 3.33 mHz. First, C_p' and C_p'' were measured during the cooling of griseofulvin melt from 370 to 335 K at 1 K/h (0.0167 K/min) rate, and these values denoted by squares are plotted against T in Figs. 2 and 3, respectively. Thereafter, the sample was heated at the same rate of 1 K/h and the C_p' and C_p'' measured during the heating are plotted as circles in Figs. 2 and 3. As is expected for a reversible relaxation, C_p' and C_p'' values in Figs. 2 and 3 measured during the cooling of the sample coincide respectively with those measured during the heating over most of the temperature range.

The C_p' against T plot in Fig. 2 shows a sigmoid shape decrease in C_p' over the 348–362 K range and the C_p'' plot in Fig. 3 shows an asymmetric peak in at 356.4±0.1 K. These features are characteristic of the variation of τ_{cal} with T for a fixed ω_{mod}, and are independent of the direction of temperature change. This demonstrates that the initial state of the

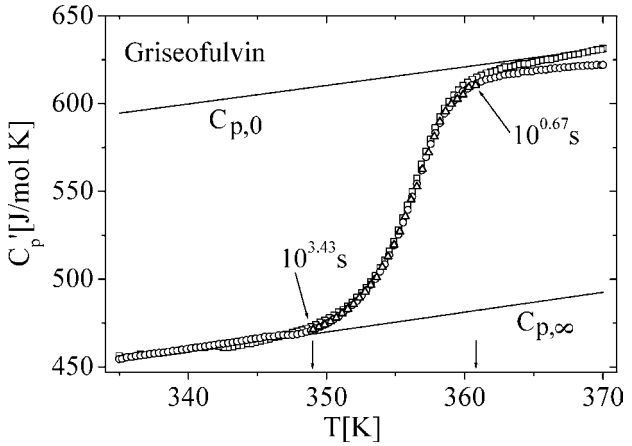

Fig. 2. The real component of the complex heat capacity, C_p', of griseofulvin measured during its cooling from 370 to 335 K and thereafter during its heating from 335 to 370 K is plotted against the temperature. The heating and cooling rates were 1 K/h (0.0167 K/min), the peak- to-peak modulation amplitude was 1 K and the modulation frequency was 3.33 mHz (modulation period of 300 s). *Open squares* show the data obtained from measurements performed during cooling and *open circles* from those performed during heating. The errors in the measurements were within (±0.25 J/(mol K)). *Open triangles* are the values calculated, as described in the text. The temperature limits (349.0 and 360.8 K) for calculating the characteristic time, τ_{cal}, are indicated. Also given are the maximum and the minimum values of τ_{cal} which were determined at the indicated temperatures. In the data in 342 to 349 K range there is small up-step near 343 K during cooling, while the heating curve returns to the "regular profile" smoothly near 348 K. This is attributed to the loss of adhesion of the glassy sample from the capillary wall. For this reason, the $C_{p,\infty}\left(C_{p,\infty}[\mathrm{J/(mol\ K)}] = 74.79 + 1.129T/K\right)$ line has been chosen as the tangent to the cooling C' curve at T>348 K. $C_{p,0}\left(C_{p,0}[\mathrm{J/(mol\ K)}] = 239.90 + 1.058T/K\right)$ is the equilibrium heat capacity. Therefore, the C_p' data at lower T has been neglected and τ_{cal} has been calculated from the cooling and from the heating curves at T>349 K, as indicated in Fig. 4.

sample was attained within one modulation cycle. Therefore, during the temperature modulation period of 300 s (ω_{mod}=3.33 mHz) at T>350 K, the structure *did not* kinetically freeze during the cooling part of the sinusoidal temperature change and the structure did not relax during the heating part. Therefore, the C_p' and C_p'' of griseofulvin measured at T>350 K are for its thermodynamic equilibrium state. At low temperatures, in the 347–352 K range of the sigmoid, C_p' and C_p'' measured during the cooling of griseofulvin shown by squares in Figs. 2 and 3 are higher than those measured during the heating of the sample, as shown by circles. The maximum difference is more than the measurement errors, as also observed earlier (16). It seems to be related to a basic feature in the formalism of TMSC, which has no effect on our analysis. Also, the plot in Fig. 2 shows that at the highest temperature of 370 K, C_p' of griseofulvin is 9.5 J/(mol K) less than the value measured after cooling the sample to 335 K and then heating to 370 K. This difference is 1.5% (9.5×100/625), which is somewhat greater than the error in the measurements. It is conceivable that impurities in our sample crystallized and phase separated. Even after this occurrence the sample did not crystallize further. It has no effect on the C_p' value in the glassy state below 342 K. As seen in Fig. 3, it also has no effect on the C_p'' value at high temperatures.

Griseofulvin is a P-type melt (30,44), i.e., its $dC_{p,0}/dT$ is positive. The T_f of its glassy state formed here by extremely slow cooling at 1 K/h rate is already much lower than that of the glass formed by cooling at a higher rate. Consequently, C_p', α and $\Delta C_{p,JG}$ of its glassy state in Eq. 1 would be even smaller than that of the state formed by cooling at 20 K/h rate, and its C_p' would have contributions mainly from phonons and anharmonic forces. As observed for C_p' of a network-structure organic glass (23), C_p' of griseofulvin at $T < T_g$ would decrease with time, but this decrease would be slow and small and, therefore, C_p' would be negligibly different from $C_{p,\infty}$.

The C_p'' peak appears at the temperature of 356.4±0.1 K in Fig. 3. At this T, τ_{cal} is equal to the reciprocal of the angular frequency, which is 20.9 mrad/s for ω_{mod} of 3.33 mHz. Thus τ_{cal} is 47.9 s for griseofulvin at 356.4 K. In order to calculate τ_{cal} at other temperatures from the C_p' and C_p'' data in Figs. 2 and 3, one needs the quantity $[C_{p,0}(T) - C_{p,\infty}(T)]$ for substituting in Eqs. 6 and 7. $C_{p,0}$ is readily determined from the upper straight line drawn in Fig. 2, and it varies little with T. To determine $C_{p,\infty}$, C_p' taken from Fig. 2 is replotted against T in Fig. 1A. It shows that C_p' of the melt at 345 K is within the experimental and extrapolation errors of $C_{p,app}$ of the glassy state, and that $C_{p,app}$ of the glassy state linearly extrapolates to C_p' of the melt at higher temperatures. Therefore, we take C_p' as equal to $C_{p,\infty}$ of the melt at a low temperatures. At higher temperatures, $C_{p,\infty}$ was determined by linear extrapolation of the $C_{p,app}$ or C_p' data for the glass, as

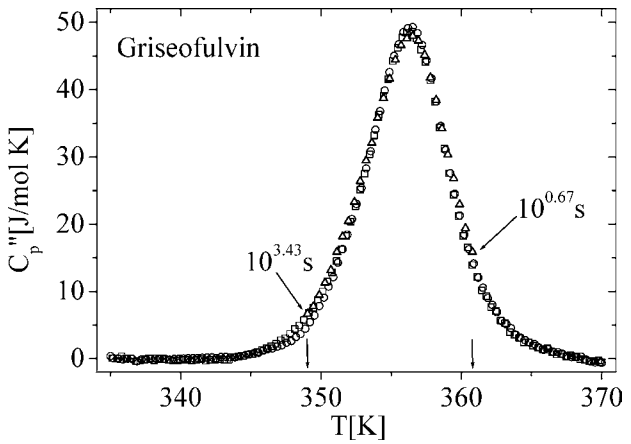

Fig. 3. The imaginary component of the complex heat capacity, C_p'', of griseofulvin measured during its cooling from 370 to 335 K and thereafter during its heating from 335 to 370 K is plotted against the temperature. The heating and cooling rates were 1 K/h (0.0167 K/min), the peak-to-peak modulation amplitude was 1 K and the modulation frequency is 3.33 mHz (modulation period of 300 s). *Open squares* show the data obtained from measurements performed during cooling and *open circles* from those performed during heating. The errors in the measurements were within 0.5%. *Open triangles* are for the values calculated, as described in the text. The temperature limits for calculating the characteristic time, τ_{cal}, are indicated. Also given are the maximum and the minimum extreme values of τ_{cal}, which was determined at these temperatures. The distribution of relaxation time parameter, β over this temperature range is 0.67.

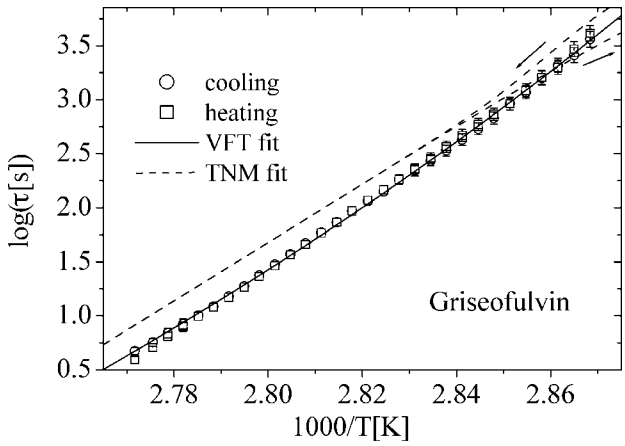

Fig. 4. The characteristic time, τ_{cal}, of griseofulvin calculated from the measured data in Figs. 1 and 2 is plotted against the reciprocal temperature during cooling (*open squares*) and during heating (*open circles*) . The *smooth full line* is the fit of the Vogel–Fulcher–Tamman equation, $\tau_{cal} = 10^{-13.3} \exp[2,292/(T - 289.5)]$. The *dashed line* is for the relaxation time calculated from the $C_{p,app}$ data shown in Fig. 1A by using the TNM's non-exponential, nonlinear structural relaxation with the values of the parameters, $\ln A = -170$, $\beta = 0.75$, $x = 0.45$ and $\Delta h^* = 516$ kJ/mol both during cooling and successive heating.

shown by the lower straight line in Fig. 2. The $[C_{p,0}(T) - C_{p,\infty}(T)]$ was then used in Eqs. 6 and 7 to calculate τ_{cal} at different T. The best fit value for β in this calculation was found to be 0.67. The τ_{cal} calculated at the uppermost and lowermost T is marked in Figs. 2 and 3. The procedure of determining $[C_{p,0}(T) - C_{p,\infty}(T)]$ makes τ_{cal} uncertain only by 1–2%. This uncertainty would increase if β varied with T.

The plot of $\log_{10}(\tau_{cal}[s])$ against $1{,}000/T$ is shown in Fig. 4, where squares denote the values calculated from the C_p' and C_p'' measured during the cooling and circles those measured during the heating. The plot is described by the Vogel–Fulcher–Tammann equation (68–70),

$$\log_{10}(\tau_{cal}[s]) = A_{VFT} + \left(\frac{B}{2.3026(T - T_0)}\right) \qquad (8)$$

with the best fit values: $A_{VFT} = -13.3$ and $B = 2292$ K and $T_p = 289.5$ K.

The effect of the temperature-independent β can be seen by recalculating C_p' and C_p'' at different T by using Eqs. 5 and 6. The calculated values are plotted as triangles in Figs. 2 and 3. The agreement noted between the calculated and measured values demonstrates that use of a fixed β value has no significant effect on τ_{cal} determined over this T range. This also confirms that griseofulvin remains in an equilibrium state at these temperatures during both the cooling and the heating at 1 K/h. For instructive purpose, we use the $C_{p,0}$, $C_{p,\infty}$, β and τ_{cal} values to simulate the isothermal relaxation spectra of C_p' and C_p'' for griseofulvin at 350 to 360 K at 2 K intervals. These spectra are shown in Fig. 5 (top and bottom), respectively.

We now turn to the analysis of the $C_{p,app}$ data plotted in Fig. 1A. It was fitted to a non-exponential, nonlinear structural relaxation formalism according to the model based on the concepts of Tool (71) and Narayanaswamy (72), as extended by Moynihan, *et al.* (73). This formalism incorporates the non-exponential character of the relaxation spectra in terms of the parameter β, with a characteristic relaxation time τ, whose infinite temperature value is A. It introduces a nonlinearity parameter x, and an activation energy Δh^*. The data fitting procedure has been described elsewhere (74,75). The best-fit parameters for $C_{p,app}$ of griseofulvin were: $\ln A = -170$, $\beta = 0.75$, $x = 0.45$ and $\Delta h^* = 516$ kJ/mol for both, during the melt's cooling to form the glassy state and during the heating to soften the glass to ultraviscous melt. The smooth lines drawn through the data points in Fig. 1A show the $C_{p,app}$ calculated by using these parameters.

For comparison with the τ_{cal} determined from C_p' and C_p''data, τ was calculated from the above-given four parameters. It is plotted as a dashed line in Fig. 4. We note a significant difference between the τ_{cal} and τ. Even though the parameter β is temperature-independent in both calculations, its value differs: 0.67 from the C_p' and C_p'' data and 0.75 for the $C_{p,app}$ data. The difference between the two analysis is that there is no structural change during the period of C_p' and C_p'' measurements but there is a structural change during the period of $C_{p,app}$ measurements which is taken into account by the parameter x in the Tool–Narayanaswamy–Moynihan formalism (71–73). Since no other approximation is made in analyzing the C_p' and C_p'', τ_{cal} determined from C_p' and C_p'' would be more reliable for estimating the molecular mobility

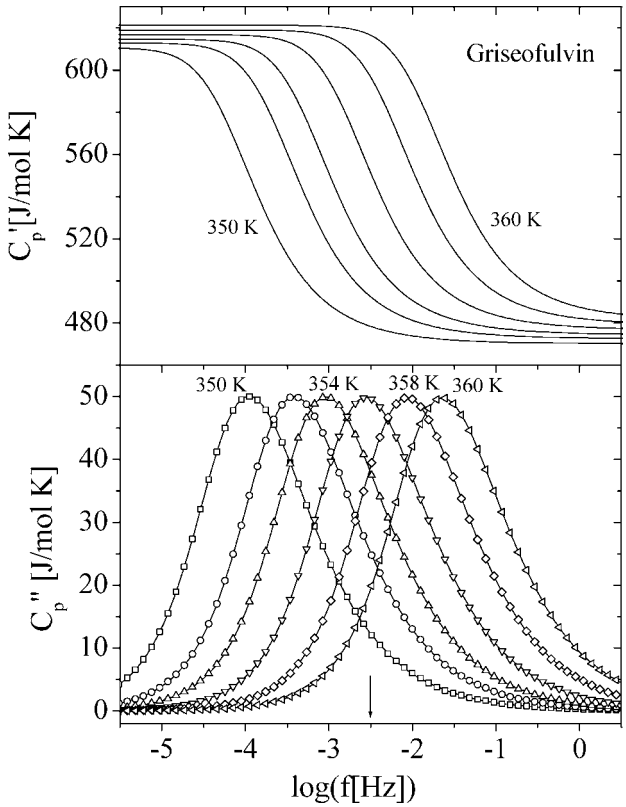

Fig. 5. The calculated C_p' and C_p'' spectra of griseofulvin at several temperatures, as determined from the parameters, $C_{p,0}$, $C_{p,\infty}$, τ_{cal} and β obtained here. The temperatures are indicated *next to the spectra*. The *arrow* indicates the fixed frequency at which the modulated calorimetric study was performed.

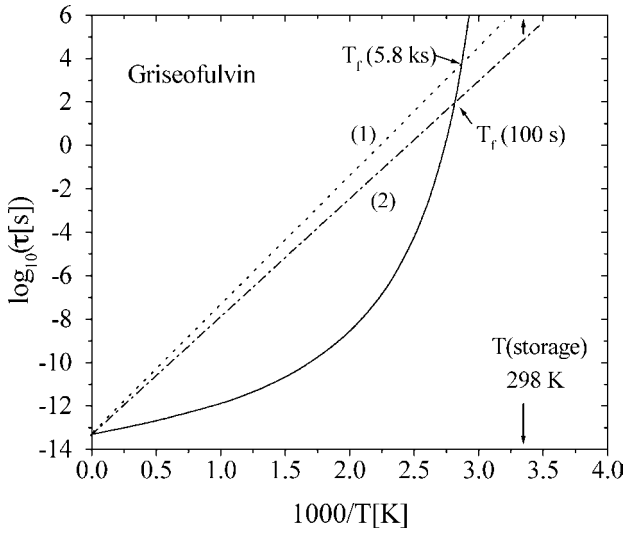

Fig. 6. The τ_{cal} calculated from the best-fit parameters of the Vogel–Fulcher–Tammann equation is plotted logarithmically against the reciprocal temperature. The *two straight line* from the origin at $1/T=0$ are for the Arrhenius plots with the Arrhenius energy that increases with decrease in the fictive temperature. *Curve 1* is for the glassy state of griseofulvin obtained by cooling at such a rate that its T_f is 347.8 K and τ_{cal} at T_f is 5.8 ks. *Curve 2* is for the glassy state of griseofulvin obtained by cooling at such a rate that its structure freezes at a T_f when its τ_{cal} is 100 s. *Small vertical arrow* indicate the direction in which τ_{cal} would increase as a consequence of structural relaxation during storage at 298 K. This would increase griseofulvin's stability against crystallization. The extrapolation limit is made evident in this figure.

in griseofulvin than τ determined by fitting the $C_{p,app}$ against T plot.

DISCUSSION

Configurational and Vibrational Heat Capacity and Entropy

In the current thermodynamics-based modeling of a pharmaceutical's stability against crystallization (12–15), $C_{p,conf}$, the configurational part of C_p is taken as equal to the excess heat capacity of a melt over that of the crystal phase, which is then used in a variety of relations between the entropy and molecular mobility or viscosity of a liquid (10,15,18). Since this equality is basically unjustifiable (29–31,43), and crystal is denser than glass, $C_{p,\mathrm{conf}}$ needs to be determined for the purpose of thermodynamically based modeling. To determine it here, we first note that according to the plot for $C_{p,app}$ in Fig. 1A, griseofulvin vitrifies at $T<343$ K during the cooling at 20 K/h [the plots of $H_{conf}(T) - H_{conf}(290\ \mathrm{K})$ and of $[S_{conf}(T) - S_{conf}(290\ \mathrm{K})$ in Fig. 1B and C show it more clearly]. At a higher T of 348 K, the calculated τ_{cal} is $10^{4.3}$ s and since ω_{mod} is 20.9 milliradian (3.33 mHz), $\omega_{mod}\tau=56.2$ and $\omega_{mod}{}^2\,\tau^2=3{,}160$, which is much greater than 1. For this condition, C_p' is close to $C_{p,\infty}$. Hence at T of ~348 K or lower, the $C_{p,\infty}\left(=C_{p,vib}+C_{p,anh}\right)$ value has been reached. Its value is ~475 J/(mol K) at 350 K. Since it is mainly due to phonons and anharmonic forces, this unusually high value indicates a relatively low vibrational (phonon) frequency and/or a large anharmonicity both expected for a large molecule. As they represent the kinetic energy of a molecules, both vibrational properties are important for its solubility and its chemical reactions.

$C_{p,conf}$ is then obtained by subtracting $C_{p,\infty}$ from $C_{p,0}$. At a temperature of 370 K, $C_{p,0}$ of griseofulvin is 627 J/(mol K) and $C_{p,\infty}$ extrapolated from C_p' of the glassy state at 370 K is ~490 J/(mol K). Thus $C_{p,conf}$, or $C_{p,\alpha}$ in Eq. 1, is ~137 J/(mol K) at 370 K. This means that $C_{p,conf}$ of griseofulvin is ~28% of the vibrational contribution $\left(=C_{p,vib}+C_{p,anh}\right)$ of 490 J/(mol K).

The slope of $C_{p,0}$ against T plot in Fig. 2 is 1.06 J/(mol K^2), and that of $C_{p,\infty}$ against T plot is 1.13 J/(mol K^2). A similarly small difference was observed between the corresponding slopes of the plots for acetaminophen in Fig. 1 (16). This small difference indicates that $C_{p,conf}$ decreases only slowly with increase in T.

Relaxation Time and Stability of Griseofulvin Glass

For an unachievable thermodynamic equilibrium state of griseofulvin at 298 K, Eq. 8 yields a τ_{cal} value of 10^{99} years. This value is misleading because the state of griseofulvin at 298 K is a non-equilibrium glass of fixed structure and T_f that were fixed at its vitrification temperature during cooling and remained fixed on further cooling to 298 K. In the non-equilibrium isostructural state, τ_{cal} varies with T according to the Arrhenius equation, $\tau_{cal}\propto\exp\left(E_{Arrh}/RT\right)$, as described earlier here and observed by a variety of experiments (32,53–57). This variation is also implicit in the Tool–Narayanswamy–Moynihan's equation (73) when T_f is kept fixed. It also follows from the Adam–Gibbs equation (9),

$$\tau_{cal}=\tau_{0,AG}\exp\left(\frac{C}{TS_{conf}}\right) \tag{9}$$

where $\tau_{0,AG}$ is the high-temperature limit of τ_{cal}, and C is a material constant in J/mol. When the glass structure does not change with changing T, S_{conf} and T_f do not change, and Eq. 9 becomes, $\tau_{cal}=\tau_{0,AG}\exp\left(constant/T\right)$, and $\log(\tau_{cal})$ varies linearly with $1/T$ as in the Arrhenius equation. Therefore, the true τ_{cal} of griseofulvin at 298 K would be much less than that estimated from Eq. 8. To determine the true τ_{cal} in the glassy state, we may rewrite Eq. 9 as,

$$\tau_{cal}=\tau_0\exp\left(\frac{E}{\phi_{structure}RT}\right) \tag{10}$$

where τ_0 is the high-temperature limit of τ_{cal} which corresponds to the phonon frequency, E is a constant with units of energy, R is the gas constant and $\phi_{structure}$ denotes the magnitude of a structure-controlled property which decreases, like S_{conf}, with decrease in T. After the kinetic freezing of the structure at $T=T_f$, further cooling increases τ_{cal} according to the relation,

$$\tau_{cal}=\tau_0\exp\left(\frac{E_{Arrh}\left(T_f\right)}{RT}\right) \tag{11}$$

where $E_{Arrh}(T_f) = E/\phi_{structure}(T_f)$, which does not change with varying T as long as $T < T_f$. Therefore,

$$E_{Arrh}(T_f) = 2.303RT_f\left[\log_{10}\tau_{cal}(T_f) - \log_{10}\tau_0\right] \qquad (12)$$

where τ_{cal} (T_f) is the measured τ_{cal} at the temperature T_f at which the structure kinetically froze. Thus the T_f -dependent E_{Arrh} is determined both by the T_f and τ_{cal} at T_f.

When a melt is cooled slowly, T_f of the glassy state formed is low and for a low T_f, τ_{cal} would be long, because the increase in $\log_{10}\tau_{cal}$ with decrease in T_f in Eq. 12 overcompensates for the decrease in T_f (percentage increase in $\log_{10}\tau_{cal}$ being much greater than the percentage decrease in T_f). Hence E_{Arrh} is high when T_f is low. In contrast, when a melt is cooled rapidly, T_f of the glassy state formed is high, τ_{cal} is shorter and E_{Arrh} in Eq. 12 would be lower. For a given material, therefore, the slope of the $\log_{10}\tau_{cal}$ against $1/T$ plot would be high when T_f is low and low when T_f is high.

We now estimate τ_{cal} of vitrified griseofulvin at the storage temperature, $T_{storage}$ by rewriting Eq. 11 as,

$$\tau_{cal}(T_{storage}) = \tau_0 \exp\left(\frac{E_{Arrh}(T_f)}{RT_{storage}}\right) \qquad (13)$$

where the T_f-dependent E_{Arrh} is given by Eq. 12. Accordingly, $\log_{10}\tau_{cal}$ $(T_{storage})$ varies linearly with $1/T_{storage}$ as long as T_f does not change.

The quantity τ_0 is equal to the vibrational time scale, which is in the 10^{-14} s range. We use $10^{-13.3}$ s for τ_0 corresponding to the already obtained A_{VFT} value of -13.3 in Eq. 8. To determine E_{Arrh} from Eq. 12 one needs T_f . It is determined by the same procedure as T_g, i.e., by using the intersection temperature of two extrapolated lines for the liquid and glass in the plots of the enthalpy and entropy against T. From the plots labeled "a" in Fig. 1B and C, T_f is 347.8 K. At this temperature τ_{cal} is 5.8×10^3 s. By substituting τ_0=$10^{-13.3}$ s and $\tau_{cal} = 5.8 \times 10^3$ s for T_f of 347.8 K in Eq. 12, we determine E_{Arrh} as 113.6 kJ/mol. Finally, by substituting τ_0 and E_{Arrh} in Eq. 13, we calculate τ_{cal} at $T_{storage}$ of 298 K. This value is 4.09×10^6 s or 1.6 months. If, instead of $10^{-13.3}$ s, we use τ_0 of 10^{-14} s, τ_{cal} would be 5.39×10^6 s or ~2.1 months. This means that the relaxation time of the griseofulvin structure at 298 K is at least ~1.6 months. It would be longer at a lower storage temperature of 277 K. If griseofulvin was vitrified by using a slower cooling rate, its T_f would be low, $\tau_{cal}(T_f)$ longer, E_{Arrh} higher and hence the relaxation time at 298 K would be longer.

If griseofulvin were to structurally relax during storage, T_f would continuously decrease with time and E_{Arrh} of the non-equilibrium state would increase. This means that not only τ_{cal} at $T_{storage}$ would increase with time but also the slope of the $\log_{10}\tau_{cal}$ against $1/T_{storage}$ plot would increase asymptotically until a time is reached when T_f has asymptotically decreased to $T_{storage}$. To show this, τ_{cal} was calculated from Eq. 8 using the fitted parameters. It is plotted as $\log_{10}(\tau_{cal})$ against $1{,}000/T$ in Fig. 6, along with two other plots, (1) the Arrhenius plot of griseofulvin's vitrified state obtained by cooling at 20 K/h with $\tau_{cal} = 5.8 \times 10^3$ s at T_f of 347.8 K and (2) an arbitrary plot for $\tau_{cal}(T_f)$ of 100 s. The vertical top arrow indicates the direction of change in τ_{cal} if griseofulvin were to structurally relax during storage at a temperature T and its T_f decreased.

The lack of crystallization of its ultraviscous melt at 370 K and also during slow cooling and heating at 1 K/h indicates that the energy barrier to nucleation of the ultraviscous melt is already high at 370 K. For that reason, the glassy state of griseofulvin would be stable at ambient temperature, thereby maintaining its bioavailability.

CONCLUSIONS

Griseofulvin does not crystallize on heating to 373 K, ~20 K above its calorimetric T_g, which is 350.6 K. The lack of crystallization of its ultraviscous melt at 370 K and on its slow cooling and heating at 1 K/h indicates that the energy barrier to nucleation of the ultraviscous melt is already high at 370 K. For that reason, the glassy state of griseofulvin would be stable at ambient temperature, thereby maintaining its bioavailability. At temperatures close to T_g, the calorimetric relaxation time has a relatively narrow distribution, with a non-exponential relaxation parameter of 0.67. This seems consistent with an earlier view that nucleation and crystal growth in molecular materials is less probable when the distribution is narrower and localized relaxation modes make a smaller contribution.

Use of different techniques for determining the molecular mobility for use in the thermodynamics-based models for stability of pharmaceuticals often leads to different conclusions, particularly when the vibrational heat capacity of a crystal and glass state are also taken to be the same. Griseofulvin's molecular mobility measured by the heat capacity relaxation eliminates the errors arising from using other techniques, especially when the vibrational heat capacity can be accurately determined. In the method used for griseofulvin, the relaxation time corresponds to the same motions that contribute to the change in thermodynamic quantities. Therefore it is more reliable for modeling the stability of a pharmaceutical against crystallization than other methods.

Basic concepts of the glass relaxation phenomena may be used to determine the true molecular mobility of a pharmaceutical at the storage temperature, and to estimate the change of the mobility with the storage time. Accordingly, the molecular relaxation time of griseofulvin is about 2 months at 298 K. It would spontaneously increase with time. If the long-range motions alone were responsible for crystallization, griseofulvin's stability against crystallization during storage would increase with time, thus maintaining most of its enhanced bioavailability.

ACKNOWLEDGEMENTS

This research was financially supported by Pfizer as part of collaborative program. The experimental part of this study was performed at CNR, IPCF Pisa.

REFERENCES

1. B. C. Hancock and G. Zografi. Characteristics and significance of the amorphous state in pharmaceutical systems. *J. Pharm. Sci.* **86**:1–12 (1997).
2. D. Q. M. Craig, P. G. Royall, V. L. Kett, and M. L. Hopton. The relevance of the amorphous state to pharmaceutical dosage forms: glassy drugs and freeze dried systems. *Int J Pharmaceut.* **179**:179–207 (1999).
3. B. C. Hancock and M. Parks. What is the true solubility advantage for amorphous pharmaceuticals?. *Pharm. Res.* **17**:397–404 (2000).
4. G. P. Johari and D. Pyke. On the glassy and supercooled states of a common medicament: Aspirin. *Phys. Chem. Chem. Phys.* **2**:5479–5484 (2000).
5. L. Yu. Amorphous pharmaceutical solids: preparation, characterization and stabilization. *Adv. Drug. Deliv. Rev.* **48**:27–42 (2001).
6. L. R. Hilden and R. Morris. Prediction of relaxation behavior of amorphous pharmaceutical compounds. I. Master curves concept and practice. *J. Pharm. Sci.* **92**:1464–1472 (2003).
7. A. M. Kaushal, P. Gupta, and A. K. Bansal. Amorphous drug delivery systems: molecular aspects, design and performance. *Crit. Rev. Ther. Drug Carrier Systems* **21**:133–193 (2004).
8. Y. C. Martin. A bioavailability score. *J. Med. Chem.* **48**:3164–3170 (2005).
9. G. Adam and J. H. Gibbs. The temperature dependence of cooperative relaxation properties in glass-forming liquids. *J. Chem. Phys.* **43**:139–146 (1965).
10. W. Kauzmann. The glassy state and the behaviour of liquids at low temperature. *Chem. Rev.* **43**:219–256 (1948).
11. B. C. Hancock, S. L. Shamblin, and G. Zografi. Molecular mobility of pharmaceutical solids below the glass transition temperature. *Pharm. Res.* **12**:799–806 (1995).
12. B. C. Hancock, K. Christensen, and S. L. Shamblin. Estimating the critical molecular mobility temperature (T_k) of amorphous pharmaceuticals. *Pharm. Res.* **15**:1649–1651 (1998).
13. S. L. Shamblin, X. Tang, L. Chang, B. C. Hancock, and M. Pikal. Characterization of the time scales of molecular motion in pharmaceutically important glasses. *J. Phys. Chem. B.* **103**:4113–4121 (1999).
14. K. J. Crowley and G. Zografi. The use of thermal methods for predicting the glass-former fragility. *Thermochim. Acta.* **380**:79–93 (2001).
15. D. Zhou, G. G. Z. Zhang, D. Law, D. J. W. Grant, and E.A. Schmitt. Physical stability of amorphous pharmaceuticals: Importance of configurational thermodynamic quantities and molecular mobility. *J. Pharm. Sci.* **91**:1863–1872 (2002).
16. E. Tombari, S. Presto, G. P. Johari, and R. M. Shanker. Dynamic heat capacity and relaxation time of ultraviscous melt and glassy acetaminophen. *J. Pharm. Sci.* **95**:1006–1021 (2006).
17. J. J. M. Ramos, R.Taveira-Marques, and H. P. Diogo. Estimation of the fragility index of indomethacin by DSC using the heating and cooling rate dependency of the glass transition. *J. Pharm. Sci.* **93**:1503–1507 (2004), and references therein.
18. G. P. Johari, S. Kim, and R. M. Shanker. Dielectric studies of molecular motions in amorphous solid and ultraviscous acetaminophen. *J. Pharm. Sci.* **94**:2207–2223 (2005).
19. A. Boller, C. Schick, and B. Wunderlich. Modulated differential scanning calorimetry in the glass transition region. *Thermochim Acta.* **266**:97–911 (1995). See also papers in Special issues on Calorimetry In *Thermochim. Acta.* volume 304–305 (year1997) and volume 377 (year 2001).
20. S. L. Simon. Temperature modulated DSC: Theory and application. *Thermochim Acta* **374**:55–71 (2001).
21. G. Salvetti, E. Tombari, L. Mikheeva, and G. P. Johari. The endothermic effects during denaturation of lysozyme by temperature modulated calorimetry and an intermediate reaction equilibrium. *J. Phys. Chem. B* **106**:6081–6087 (2002).
22. E. Tombari, G. Salvetti, C. Ferrari, and G. P. Johari. Structural unfreezing and endothermic effects in liquids, β-D-fructose. *J. Phys. Chem. B.* **108**:16877–16882 (2004).
23. E. Tombari, S. Presto, G. Salvetti, and G. P. Johari. Spontaneous decrease in the heat capacity of a glass. *J. Chem. Phys.* **117**:8436–8441 (2002).
24. G. P. Johari, C. Ferrari, E. Tombari, and G. Salvetti. Temperature modulation effects on a material's properties: Thermodynamics and dielectric relaxation during polymerization. *J. Chem. Phys.* **110**:11592–11598 (1999).
25. J. Wang and G. P. Johari. Effects of sinusoidal temperature and pressure modulations on the structural relaxation of amorphous solids. *J. Non-Cryst. Solids* **281**:91–107 (2001).
26. K. L. Ngai and M. Paluch. Classification of secondary relaxation in glass-formers based on dynamic properties. *J. Chem. Phys.* **120**:857–873 (2004).
27. M. Goldstein. Viscous liquids and the glass transition V. Sources of excess specific heat of the liquid. *J. Chem. Phys.* **64**:4767–4774 (1976).
28. G. P. Johari. On the excess entropy of disordered solids. *Phil. Mag. B.* **41**:41–47 (1981).
29. G. P. Johari. Contributions to the entropy of a glass and liquid, and the dielectric relaxation time. *J. Chem. Phys.* **112**:7518–7523 (2000).
30. G. P. Johari. On extrapolating a supercooled liquid's excess entropy, the vibrational component, and interpreting the configurational entropy theory. *J. Phys. Chem. B.* **105**:3600–3604 (2001).
31. G. P. Johari. Decrease in the configurational and vibrational entropies on supercooling a liquid and their relations with the excess entropy. *J. Non-Cryst. Solids* **307–310**:387–392 (2002).
32. G. W. Scherer. *Relaxation in glass and composites*, Wiley, New York, 1986, pp. 113–174.
33. G. P. Johari. Glass transition and secondary relaxation in molecular liquids and crystals. *Ann. NY. Acad. Sci.* **279**:117–140 (1976).
34. J. Haddad and M. Goldstein. Viscous liquids and the glass transition. VIII. Effect of fictive temperature on dielectric relaxation in the glassy state. *J. Non-Cryst. Solids* **30**:1–22 (1978).
35. G. P. Johari. Effects on annealing on the secondary relaxations in glass. *J. Chem. Phys.* **77**:4619–4626 (1982).
36. H. Wagner and R. Richert. Equilibrium and non-equilibrium type β-relaxations: D-sorbitol *versus o*-terphenyl. *J. Phys. Chem.* **103**:4071–4077 (1999).
37. G. P. Johari and M. Goldstein. Viscous liquids and the glass transition. II. Secondary relaxations in glasses of rigid molecules. *J. Chem. Phys.* **53**:2372–2388 (1970).
38. G. P. Johari. Intrinsic mobility of molecular glasses. *J. Chem. Phys.* **58**:1766–1770 (1973).
39. G. P. Johari, G. Power, and J. K. Vij. Localized relaxation's strength and its mimicry of glass-softening thermodynamics. *J. Chem. Phys.* **116**:5908–5909 (2002).
40. G. P. Johari, G. Power, and J. K. Vij. Localized relaxation in a glass and the minimum in its orientational polarization contribution. *J. Chem. Phys.* **117**:1714–1722 (2002).
41. G. Power, G. P. Johari, and J. K. Vij. Relaxation strength and localized motions in D-sorbitol and mimicry of glass-softening thermodynamics. *J. Chem. Phys.* **119**:435–442 (2003).
42. G. Power, J. K. Vij, and G. P. Johari. Kinetics of spontaneous change in the localized motions of D-sorbitol glass. *J. Chem. Phys.* **124**:074509 (8 pages) (2006).
43. G. P. Johari. The entropy loss on supercooling a liquid and anharmonic contributions. *J. Chem. Phys.* **116**:2043–2046 (2002).
44. G. P. Johari. An equilibrium supercooled liquid's entropy and enthalpy in the Kauzmann and the third law extrapolations and a proposed experimental resolution. *J. Chem. Phys.* **113**:751–761 (2000).
45. G. P. Johari. Examining the entropy theory's application for viscosity data and the inference for a thermodynamic transition in an equilibrium liquid. *J. Non-Cryst. Solids* **288**:148–158 (2001).
46. G. P. Johari. Heat capacity and entropy of an equilibrium liquid from T_g to 0 K, and examining the conjectures of an underlying thermodynamic transition. *Chem. Phys.* **265**:217–231 (2001).
47. G. P. Johari. Use of crystal polymorphs for resolving an equilibrium liquid's state on supercooling to 0 K. *J. Chem. Phys.* **116**:1744–1747 (2002).
48. K. Kishimoto, H. Suga, and S. Seki. Calorimetric study of the glassy state. VIII. Heat capacity and relaxation phenomena of isopropylbenzene. *Bull. Chem. Soc. Jap.* **46**:3020–3031 (1973).

49. H. Fujimori and M. Oguni. Calorimetric Study of D, L-propene carbonate: Observation of the beta- as well as alpha-glass transition in the supercooled liquid. *J. Chem. Thermodyn.* **26**:367–378 (1994).
50. H. Fujimori, M. Muzikami, and M. Oguni. Calorimetric study of 1,3-diphenyl-1,1,3,4-tyetramethyldisiloxane: Emergence of α-, and β-, and crystalline glass transitions. *J. Non-Cryst. Solids* **204**:38–45 (1996).
51. N. G. McCrum, B. E. Read, and G. Williams. *Anelastic and Dielectric Effects in Polymeric Solids*, Wiley, New York, 1967.
52. R. L. Leheny, N. Menon, S. R. Nagel, D. L. Price, K. Suzuya, and P. Thiyagarajan. Structural studies of an organic liquid through the glass transition. *J. Chem. Phys.* **105**:7783–7794 (1996).
53. S. S. Tsao and F. Spaepen. Effects of annealing on the isoconfigurational flow of a metallic glass. *Acta Metallurgica* **33**:891–895 (1985).
54. J. Perez. *Physique et mécanique des polymères amorphes*, Lavoisier (Tec & Doc), Paris, 1992.
55. S. V. Nemilov. *Thermodynamic and kinetic aspects of the vitreous state*, CRC, Boca Raton, 1995.
56. E. Donth. *The Glass Transition Relaxation Dynamics in Liquids and Disordered Materials: Springer Series in Materials Science*, Springer, Berlin, 2001.
57. N. Menon, S. R. Nagel, and D. C. Venerus. Dynamic viscosity of a simple glass-forming liquid. *Phys. Rev. Lett.* **73**:963–966 (1994).
58. M. Vasanthavada, W. Q. Tong, Y. Joshi, and K. M. Serpil. Phase behavior of amorphous molecular dispersions II: Role of hydrogen bonding in solid solubility and phase separation kinetics. *Pharm. Res.* **22**:440–448 (2005).
59. A. A. Elamin, C. Ahlneck, G. Alderborn, and C. Nystrom. Increased metastable solubility of milled griseofulvin, depending on the formation of a disordered surface structure. *Int. J. Pharm.* **111**:159–170 (1994).
60. G. Salvetti, C. Cardelli, C. Ferrari, and E. Tombari. A modulated adiabatic scanning calorimeter (MASC). *Thermochim Acta.* **364**:11–22 (2000).
61. G. P. Johari, E. Tombari, S. Presto, and G. Salvetti. Experimental evidence for the heat capacity maximum during a melt's polymerization. *J. Chem. Phys.* **117**:5086–5091 (2002).
62. E. Tombari, S. Presto, G. Salvetti, and G. P. Johari. Endothermic freezing on heating and exothermic melting on cooling. *J. Chem. Phys.* **123**:051104 (4 pages) (2005).
63. E. Tombari, C. Ferrari, G. Salvetti, and G. P. Johari. Position-dependent energy of water molecules in nanoconfined water. *Phys. Chem. Chem. Phys.* **7**:3407–3411 (2005).
64. E. Tombari, C. Ferrari, G. Salvetti, and G. P. Johari. Heat capacity of tetrahydrofuran clathrate hydrate and of its components, and the clathrate formation from supercooled melt. *J. Chem. Phys.* **124**:154507 (10 pages) (2006).
65. E. Tombari, G. Salvetti, C. Ferrari, and G. P. Johari. Kinetics and thermodynamics of sucrose hydrolysis from real time enthalpy and heat capacity measurements. *J. Phys. Chem. B.* **111**:496–501 (2007).
66. E. Tombari, C. Ferrari, G. Salvetti, and G. P. Johari. Spontaneous liquifaction of isomerizable molecular crystals. *J. Chem. Phys.* **126**:021107 (4 pages) (2007).
67. R. O. Davies and G. O. Jones. Thermodynamic and kinetic properties of glasses. *Adv. Phys.* **2**:370–410 (1953).
68. H. Vogel. The law of relation between the viscosity of liquids and the temperature. *Phys. Z.* **22**:645–646 (1921).
69. G. S. Fulcher. Analysis of recent measurements of the viscosity of glasses. *J. Am. Ceram. Soc.* **8**:339–355 (1925).
70. G. Tammann and W. Hesse. Die abhangigkeit der viskositat von der temperature bei unterkuhlten flussigkeiten. *Z. Anorg. Allg. Chem.* **156**:245–257 (1926).
71. A. Q. Tool. Relation between inelastic deformability and thermal expansion of glass in its annealing range. *J. Am. Ceram. Soc.* **29**:240–253 (1946).
72. O. S. Narayanaswamy. A model of structural relaxation in glasses. *J. Am. Ceram. Soc* **54**:491–498 (1971).
73. C. T. Moynihan, P. B. Macedo, C. J. Montrose, P. K. Gupta, M. A. Debolt, J. F. Dill, B. E. Dom, P. W. Drake, A. J. Easteal, P. B. Eltermann, R. A. Moeller, H. Sasabe, and J. A. Wilder. Structural relaxation in vitreous materials. *Ann. N.Y. Acad. Sci.* **279**:15–36 (1976).
74. W. Pascheto, M. G. Parthun, A. Hallbrucker, and G. P. Johari. Calorimetric studies of structural relaxation in $AgI–AgPO_3$ glasses. *J. Non-Cryst. Solids* **171**:182–190 (1994).
75. L. Gunawan, G. P. Johari, and R. M. Shanker. Structural relaxation of acetaminophen glass. *Pharm. Res.* **23**:967–979 (2006).